Liquid Crystals
Publication details, including instructions for authors and subscription information:
http://www.informaworld.com/smpp/title~content=t713926090

Studies on the texture of nematic solutions of a rod-like polymer 1. Distortion of the director field in a magnetic field

Beibei Diao; Guy C. Berry

Online publication date: 29 June 2010

To cite this Article Diao, Beibei and Berry, Guy C.(1997) 'Studies on the texture of nematic solutions of a rod-like polymer 1. Distortion of the director field in a magnetic field', Liquid Crystals, 22: 3, 225 — 238
To link to this Article: DOI: 10.1080/026782997209270
URL: http://dx.doi.org/10.1080/026782997209270

LIQUID CRYSTALS, 1997, VOL. 22, NO. 3, 225–238

Studies on the texture of nematic solutions of a rod-like polymer 1. Distortion of the director field in a magnetic field

by BEIBEI DIAO† and GUY C. BERRY*
Department of Chemistry, Carnegie Mellon University, Pittsburgh, PA 15213, U.S.A.

(*Received 15 September 1995; in final form 2 May 1996; accepted 5 May 1996*)

The growth of the distortion of the director in an external field, and its relaxation on removal of the field are studied for nematic solutions of the rod-like poly(1,4-phenylene-2,6-benzobisthiazole), PBZT, over a range of concentration, polymer molecular weight and temperature. The twist viscosity and the order parameter are more weakly dependent on concentration than predicted for charged rod-like chains. This behaviour implies a short-range translational order in a direction orthogonal to the chain axis, induced by electrostatic interactions among the polycations on protonated PBZT. The relaxation gives a normal temperature dependence for the splay curvature elasticity, but that for the twist curvature is unexpectedly strong. This behaviour is interpreted as a weakening of the surface anchoring with increased temperature.

1. Introduction

The distortion of the director field **n** in the presence of an external magnetic field is discussed in the following for nematic solutions of the rod-like poly(1,4-phenylene-2,6-benzobisthiazole). With these solutions, the nematic order develops as the chain axes tend to become parallel, with the average direction of the axes in an ordered region at position **r** given by **n**(**r**). Although the viscoelastic behaviour of nematic polymers remains poorly understood, a rich theoretical literature is available on the anisotropic viscous behaviour of nematic fluids, and the anisotropic elasticity induced by deviations of **n**(**r**) from a distortion-free field [1–5]. For example, continuum mechanical considerations lead to expressions for the stress tensor in terms of six material parameters α_i called the Leslie–Ericksen constants ($i=1$–6) and a distortion free energy taken to be the sum of contributions $F_{\text{bulk}}(\mathbf{r})$ from the bulk [4–6] and $F_{\text{surface}}(\mathbf{r})$ from the surface [5, 7]. For weak distortions of the director field $F_{\text{bulk}}(\mathbf{r})$ is expressed in terms of the Frank curvature elasticities K_μ, with $\mu = \text{S}$, T and B for splay, twist and bend distortions, respectively [2, 3, 5, 6, 8]. The surface free energy is discussed below. Time constants associated with the development of these distortions may be used to define corresponding distortion viscosities $\eta_\mu > 0$ in terms of the α_i [2, 6]:

$$\eta_{\text{T}} = \alpha_3 - \alpha_2 \tag{1}$$

$$\eta_{\text{S}} = \eta_{\text{T}} - 2\alpha_3^2/\eta_{\text{b}} \tag{2}$$

$$\eta_{\text{B}} = \eta_{\text{T}} - 2\alpha_2^2/\eta_{\text{c}} \tag{3}$$

with $\eta_{\text{b}} = (\alpha_3 + \alpha_4 + \alpha_6)/2 > 0$ and $\eta_{\text{c}} = (\alpha_4 + \alpha_5 - \alpha_2)/2 = \eta_{\text{b}} - (\alpha_2 + \alpha_3) > 0$ being two of the three Miesowicz viscosities for flow with fixed director.

Study of the distortion of the director in an external field has been used to determine the parameters K_μ and η_μ for a number of small molecule liquid crystals [2, 5, 6, 9], with a smaller number of studies on polymeric liquid crystals [10–16]. Static and dynamic light scattering have been used to determine K_μ and values of η_μ/K_μ for both small molecule [17–20] and polymeric nematics [21–25]. In this work, an external magnetic field is applied to study the growth of the distortion for nematic solutions of a rod-like polymer, and the relaxation of the distortion on subsequent removal of the field. Defect-free preparations of the material in a homogeneous planar slab configuration are subjected to two different distortion geometries: (i) twist distortion, with an external magnetic field in the plane of the slab, and (ii) splay distortion, with an external magnetic field in a plane defined by the director and the normal to the slab. As discussed below, data on the growth and relaxation of the director field in these geometries provides information on K_{S}, K_{T} and η_{T}. One of the principal features of the deformation of nematic fluids is a coupling between the flow and the director field, resulting in complex behaviour, and unstable flow leading to an inhomogeneous velocity field [2, 5, 6]. Conversely, attempts to

*Author for correspondence.
†Present address: du Pont Co., Inc., Buffalo, NY, U.S.A.

0267–8292/97 $12·00

distort the director field by an external field (for example, a magnetic field, a thermal field, etc.) can induce a macroscopic flow coupled with the distortion. The latter behaviour will be discussed briefly, but is avoided in this study.

2. Experimental

2.1. *Materials*

Nematic solutions of poly(1,4-phenylene-2,6-benzobisthiazole), PBZT, were used in this study:

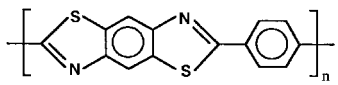

PBZT

The specifications of the PBZT used are given in table 1; L_w therein is the weight average contour length, calculated from the weight average molecular weight M_w as M_w/M_L, with $M_L = M/L$ the mass per unit length for a chain with molecular weight M and contour length L. Concentration c is expressed as wt vol^{-1}, for example, g ml^{-1}. The intrinsic viscosity $[\eta]$ in units of ml g^{-1}, is defined as usual [26], i.e. the limiting value of $(\eta_{rel}-1)/c$ at infinite dilution, with η_{rel} the relative viscosity. Polymers used were dried under vacuum prior to use. Nematic solutions were prepared by addition of the appropriate quantities of dry polymer and (99 per cent pure) methane sulphonic acid (Aldrich Chemical Company) in a 35 ml centrifuge tube containing a Teflon coated magnetic stirring bar. Slow stirring action was achieved by rotating the sample tube, between the poles of a horseshoe magnet for about 2 weeks. The solutions were stored in a vacuum over a desiccant for at least a month before being used. The steady state shear viscosity η_{ss} of the solution in the slow flow (or region II flow) for which η_{ss} is essentially independent of the shear rate [27, 28] is included in table 1 for reference.

Defect-free monodomain specimens were prepared by procedures described elsewhere [29–31]. Briefly, the cell comprised a section of rectangular Pyrex tubing (Vitro Dynamics, Rockway, NJ) terminated on either end by Leur^{TM} fitting tips. The rectangular section was 1 to 1·5 cm long, about 5 mm wide, and could be fabricated from tubing over a range of thickness; sections with 200, 300, 400, and 700 μm thickness were used in this study. The nematic sample was extruded into the cell, and the ends were closed with Leur^{TM} fitting caps. The cap assembly was coated with an epoxy resin to insure a good seal against contamination by moisture, and the cell was placed in a magnetic field (7 T) within an hour of being filled, with the long axis (i.e., the flow axis) of the cell aligned in the direction of the field. Prompt placement in the magnetic field is necessary to prevent the formation of a population of extraordinarily stable ellipsoidal shaped defect structures [29, 31].

2.2. *Methods*

A Cartesian coordinate system with the unperturbed director along the x axis ($\mathbf{n}_o = [1,0,0]$) and the nematic slab in the xy-plane will be used to describe the distortion, with the coordinate origin at midplane, so that $-d/2 \leqslant z \leqslant d/2$, with d the thickness of the slab. In this coordinate system the magnetic field is given by (i) $\mathbf{H} = [H\cos\vartheta_{mag},\ H\sin\vartheta_{mag}, 0]$ for the twist distortion, and (ii) $\mathbf{H} = [H\cos(\varphi_{mag}), 0, H\sin(\varphi_{mag})]$ for the splay distortion. As elaborated in the Appendix, with certain simplifying assumptions, the distortion of the director field in these coordinates is given by $\mathbf{n} = [\cos\vartheta(z,t), \sin\vartheta(z,t), 0]$ in the twist geometry, and by $\mathbf{n} = [\cos\varphi(z,t), 0, \sin\varphi(z,t)]$ in the splay geometry. A 7 tesla magnetic field was used in all experiments; the temperature was $22 \pm 0{\cdot}2$°C in the bore. A jig in the centre of the bore permitted the use of up to eight samples at predetermined angles ϑ_{mag} or φ_{mag}. During growth of the director field distortion, the sample was periodically removed from the magnetic field to the microscope for a short period (≈10 min) for observation. As shown below, the very

Table 1. Parameters for nematic solutions of PBZT.

Weight fraction, w	Contour length, L_w/nm	$[\eta]$/ml g^{-1}	η_{ss}/Pa s (slow flow)	T_{NI}/°C	c/c_{NI}	Cell thickness used/μm
0·0451	105	900	2700	85	1·13	300
0·0510	105	900	2400	—	1·28	400
0·0506	135	1400	25000	100	1·53	300
0·0486	145	1560	60000	100	1·50	200, 400
0·0333	155	1800	3000	62	1·38	300, 700
0·0510	155	1800	—	—	1·65	300
0·0533	155	1800	1000	105	1·72	200, 400
0·0581	155	1800	150	117·5	1·87	300
0·068	155	1800	30	—	2·19	200
0·049	155	1800	2000	—	1·47	200
0·053	155	1800	20000	—	1·71	200, 400

torpid relaxation permitted this expedient without discernible effect on the measurement. The distortion was determined as a function of the elapsed time in the magnetic field, for several sample thicknesses in some cases. Following termination of the growth of the distortion in the magnetic field, samples were placed in an oven at the desired temperature, to be removed periodically for observation.

2.3. *Conoscopic microscopy*

The distortion of the nematic was determined by observation of the conoscopic interference figures, following procedures described elsewhere [32, 33]. Prior to use, samples were confirmed to be free of defects by inspection under crossed polars in a microscope, and to give undistorted conoscopic interference figures. In conoscopy, the optic axis of nematics makes an angle of 45° with the polarizer. A polarized He–Ne laser with wave length 632·8 nm was used as a light source. The optical train on the Leitz polarizing microscope used consisted of a converging lens, the sample, an objective (×32), with a numerical aperture $\Gamma_{NA} = 0{\cdot}65$ matched to the converging lens, an analyser, and a Bertrand lens. The conoscopic interference figures were monitored and recorded on video tape using a charge-coupled device camera connected with a video monitor. Photographs of the monitor screen were made at selected times for later use.

The conoscopic fringe pattern for the undistorted nematic has been used to estimate n_E and n_O of nematic solutions of PBZT in MSA [32, 33]. Thus, as shown in the Appendix, the principal isochromates, or curves of minimum intensity, represent curves for which the retardation $\Delta\varphi$ is an integral multiple of π. An observed radial position r on the interference pattern corresponds to a refraction angle β in the medium given by

$$\frac{r}{R} = \left(\frac{\tilde{n}}{\Gamma_{NA}}\right)\sin(\beta) \tag{4}$$

with R the radius of the illuminated area, Γ_{NA} the numerical aperture of the objective lens ($\Gamma_{NA} = 0{\cdot}6$ here), and $\tilde{n} = (n_O + n_E)/2$. The refraction angle between any two adjacent fringes may be used to determine the birefringence Δn [32, 33]. The observable translation Δ of the centre of the fringe pattern from the optic axis of the microscope and its angle of rotation Ω are related to the tilt of the director with respect to the plane of the surface and its rotation in that plane, respectively. As discussed in the Appendix, the retardation in the k_x–k_y plane of the **k**-space of the interference figures may be calculated to relate Δ and Ω to certain averages of the distortion angles through the sample thickness. For pure twist ($\varphi = 0$), the observed rotation angle Ω of the fringe pattern gives $\Omega \approx C_\Omega \vartheta_{mid}$. For pure splay ($\vartheta = 0$), with $\varphi = \varphi_{mid}\cos(\pi z/d)$, the ratio of the observed results displacement Δ of the fringe pattern to the radius R of the illuminated area is given by

$$\frac{\Delta}{R} \approx C_\Delta\left(\frac{n}{\Gamma_{NA}}\right)\sin(\varphi_{mid}) \approx C_\Delta\left(\frac{n}{\Gamma_{NA}}\right)\varphi_{mid}. \tag{5}$$

Since only relative changes in the interference figures are needed here, the values of the proportionality factors C_Ω and C_Δ are not critical (see the Appendix).

Measurements of Δ/R and Ω were made from photographic images of the fringe pattern as it evolved during growth under the action of the applied field, or as it relaxed subsequent to permanent removal from the field. Slides prepared from the images were projected on a screen to facilitate accurate measurements. An image of the undistorted interference figure served as a reference for measurements. Data were reproducible to $\pm 0{\cdot}1°$ for Ω, and $\pm 0{\cdot}01$ for Δ/R.

3. Results

The birefringence Δn and $\Delta n/c$ are given as a function of the reduced concentration c/c_{NI} in figure 1, including data from reference [33] on one of the polymers used in this study. Here c_{NI} is the concentration for the first appearance of an ordered phase; since the concentration range for the biphasic gap is very small, c_{NI} may be taken as the concentration for the formation of the nematic phase for purposes here. As in the prior work, the birefringence is found to be essentially linear in c/c_{NI}. The source of the apparently systematic deviations between the data for the two studies is unknown.

Typical results for the growth and relaxation of the director field as monitored by the observables Δ for twist and Ω for splay are shown in figure 2. For reasons discussed in the following, the data are expressed as $\ln\{1 - \psi_\mu(t)/\psi_\mu(\infty)\}$ versus the elapsed time t in the magnetic field during growth of the distortion, and $\ln\{\psi_\mu(t)/\psi_\mu(\infty)\}$ versus the elapsed time t following removal from the magnetic field during relaxation, where $\psi(t) \propto \vartheta_{mid}(t) \propto \Omega(t)$ for twist or $\psi(t) \propto \varphi_{mid}(t) \propto \Delta(t)$ for splay.

As developed in the Appendix, for the large field strengths of interest here, during growth of small distortions in the director field in an external magnetic field, the distortion angle at mid-plane is given by

$$\psi_{mid}(H, \psi_{mag}, t) \approx \psi_{max}(H, \psi_{mag})[1 - \exp(-\Delta\chi H^2 t/\eta_T)] \tag{6}$$

for either small splay ($\psi = \varphi$) or twist ($\psi = \vartheta$) distortions, where $\psi_{max}(H, \psi_{mag})$ is the equilibrium distortion, t is the elapsed time, and $\Delta\chi$ is the anisotropic magnetic susceptibility. Thus, $\ln\{1 - \psi_{mid}(t)/\psi_{max}(\infty)\}$ is expected to be linear in t, where $\vartheta_{mid}(t)/\vartheta_{max}(\infty) \approx \Omega(t)/\Omega(\infty)$ and

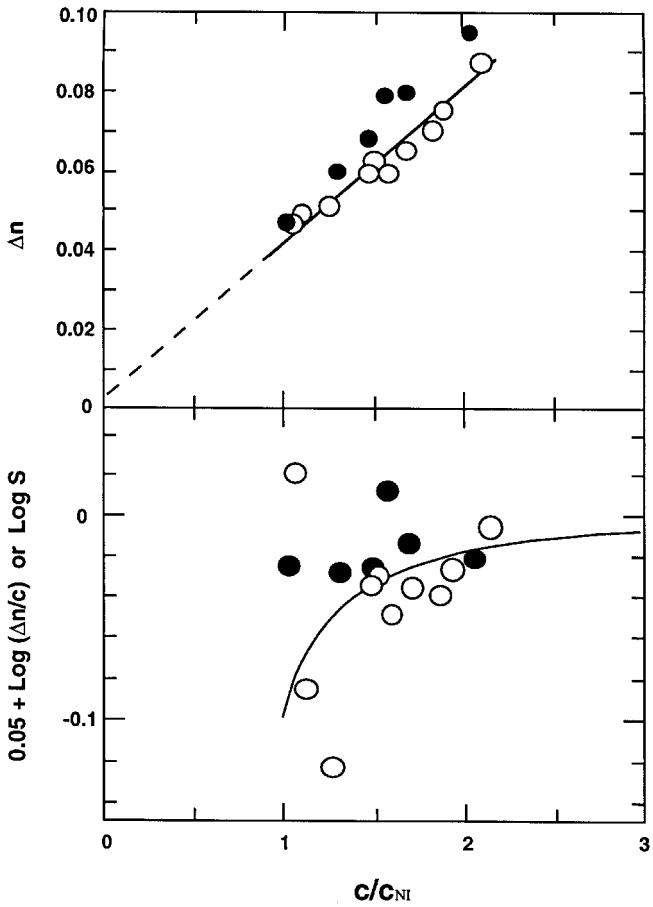

Figure 1. The birefringence Δn as function of concentration relative to the concentration c_{NI} for the order–disorder transition for nematic solutions of poly(1,4-phenylene-2,6-benzobisthiazole) in methane sulphonic acid. The filled and unfilled symbols give data from reference [33] and this study, respectively. The curve in the lower panel gives the logarithm of the order parameter given by theory as discussed in the text.

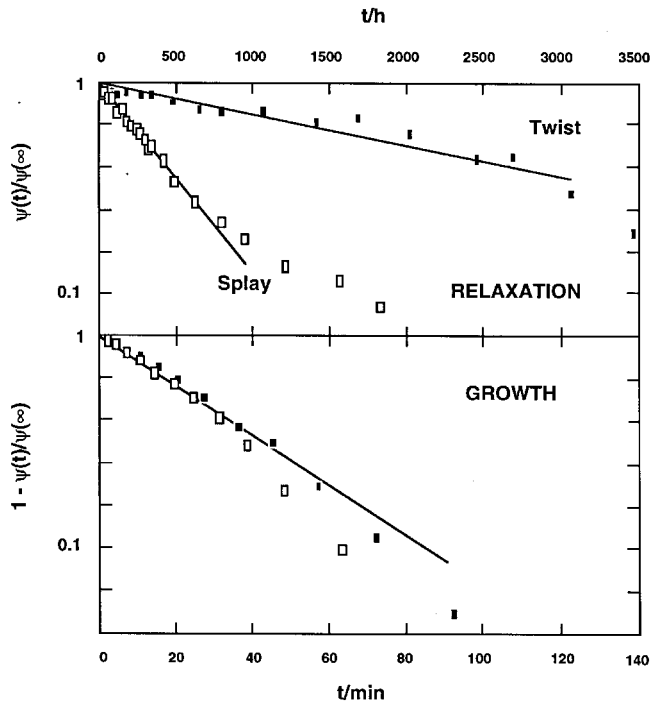

Figure 2. The growth of the distortion of the director field in an external magnetic field (7 T) (lower) and the relaxation of the distortion on removal of the magnetic field (upper) for splay and twist distortions of a monodomain nematic solution of PBZT in methane sulphonic acid (200 μm thick cell; $c = 0{\cdot}0889\,\mathrm{g\,ml^{-1}}$, $L_w = 155\,\mathrm{nm}$). The magnetic field was oriented at 7·5 and 30 degrees from the director of the monodomain for the splay and twist distortions, respectively. The average distortion $\psi(t)$ was determined in conoscopic microscopy, with $\psi(\infty)$ the value of $\psi(t)$ after a long time in the magnetic field (ψ is proportional to ϑ_{mid} in twist and φ_{mid} in splay distortions, respectively).

$\varphi(t)/\varphi(\infty) \approx \Delta(t)/\Delta(\infty)$. In either case, the tangent gives $\Delta\chi H^2 t/\eta_T$. Values of $\eta_T/\Delta\chi$ computed from the initial growth rate of the distortion are given in table 2.

On removal of the external field, the director relaxes to its unperturbed state. To a reasonable approximation, the relaxation is exponential, with [6] (see the Appendix)

$$\psi_{mid}(t - t_g) \approx \psi_{mid}(t_g) \exp[-(t - t_g)/\tau_\mu] \qquad (7)$$

where t_g is the duration of the growth of the distortion, $t - t_g$ is the elapsed time from the time the magnetic field is removed and $\tau_\mu = d^2\eta_T/\pi^2 K_\mu$. Thus, $\ln\{\psi_{mid}(t - t_g)/\psi_{mid}(t_g)\}$ is expected to be linear in t, where $\vartheta_{mid}(t - t_g)/\vartheta_{mid}(t_g) \approx \Omega(t - t_g)/\Omega(t_g)$ and $\varphi_{mid}(t - t_g)/\varphi_{mid}(t_g) \approx \Delta(t - t_g)/\Delta(t_g)$. The example given in figure 2 shows the expected exponential relaxation, with $\tau_T > \tau_S$. Values of η_T/K_T and η_T/K_S determined from τ_T and τ_S, respectively, are given in table 2.

Although it will not be pursued here, it is noted that the homogeneous distortion discussed above is not maintained for the magnetic field strengths used here with nematic solutions of PBZT if ϑ_{mag} or φ_{mag} exceeds about $\pi/4$, with the distortion becoming coupled with flow, and the creation of a *phase grating* [29]. If this behaviour persisted for smaller field strengths, it would preclude the determination of $K_T/\Delta\chi$ or $K_S/\Delta\chi$ from the critical field $H_{c,\mu}$ required for the onset of the distortion, even if the response time were more convenient. The phase grating consists of cylindrically symmetric distortions of the director out of the sample plane and toward the magnetic field, creating a grating of cylindrical lenses with axes in the sample plane, and orthogonal to $\mathbf{n}_o$. The phase grating will focus light polarized along $\mathbf{n}_o$ in bright stripes above the sample plane, with a similar plane of virtual images symmetrically placed below the sample plane. A similar phase grating has been reported for distortions in an electric field [34], and studied

Table 2. Distortion viscosities and elasticities for nematic solutions of PBZT.

c/g ml^{-1}	c/c_{NI}	η_T/K_T/(Pa s/pN) TR[a]	η_T/K_S/(Pa s/pN) SR[a]	K_S/K_T	η_T/χ_a/(s T^2) TG[a]	η_T/χ_a/(s T^2) SG[a]
0·0667[b]	1·128	200	—	—	6400	—
0·0755	1·275	1250	125	10·0	5900	7800
0·0749	1·533	1600	345	4·64	15000	20000
0·0719	1·495	1890	535	3·53	44100	47000
0·0493	1·074	3320	680	4·88	180000	163000
0·0740	1·613	2140	565	3·79	64600	70400
0·0755[b]	1·645	4660	—	—	123000	—
0·0789	1·719	1960	—	—	—	—
0·0860	1·874	—	420	—	—	—
0·0889	1·939	1970	400	4·93	48100	48500
0·0987	2·152	1550	360	4·31	112000	114000

[a] TR and SR signify data from the relaxation of twist and splay distortions, respectively, and TG and SG indicate data from the growth of twist and splay distortions, respectively.
[b] From reference [29] after correction.

theoretically within the Ericksen–Leslie constitutive relation [35].

4. Discussion

In general, for $c > c_{NI}$ the birefringence may be expressed in the form [2, 5, 6]

$$\Delta n \approx (\Delta n/\rho)^{\circ} c S \tag{8}$$

where S is the order parameter for the nematic, and this form assumes that the intrinsic anisotropic molecular optical polarizability is invariant with c. The functions $\log(\Delta n/c)$ from the results reported here, and $\log(S)$ calculated for rods interacting through a hard-core potential are shown versus c/c_{NI} in figure 1, where the data for $\log(\Delta n/c)$ are translated along the ordinate to attain approximate agreement with $\log(S)$. The theoretical treatments give numerical results [23, 24, 36] that may be represented by the semi-empirical expression [25, 37]

$$(1-S)^{1/2} S^2 / r_S \approx (3\pi)^{1/2}/8 (c/c_{NI}) \tag{9a}$$

and

$$r_S = 1 - (4/3)(1-S)[1 - k_r(1-S)] \tag{9b}$$

with $k_r = 0{\cdot}2315$, where the form of these expressions is suggested by perturbation expansions [38, 39]. With the use of these relations, $1 - S^2 \approx 1/3 (c/c_{NI})^2$. As seen in figure 1, with the exception of two points, the results obtained here, along with the data from reference [33], suggest that $\Delta n/c$ is nearly invariant over the concentration range studied, with the data consistent with the estimates $S \approx 0{\cdot}95$ and $(\Delta n/\rho)^{\circ} \approx 1$. By contrast, for the hard-core model, S is expected to increase from $\approx 0{\cdot}85$ to $\approx 0{\cdot}98$ over the range of c/c_{NI} studied; see the solid curve in figure 1.

The unexpected constancy of S over the range of c/c_{NI} studied might reflect the fact that PBZT is protonated in solution in protic acids such as MSA, becoming a polycation in solution [40]. Self-protonation of the protic acids provides cations and anions that screen the electrostatic interactions among the polycations, with MSA being a solvent of moderate ionic strength [41]. Similar effects have been noted for nematic solutions of poly(1,4-phenylene terephthalate) in sulphuric acid [42]. The thermodynamic diameter d_T provides a measure of the scale for electostatic interactions. For rod-like chains, the second virial coefficient A_2 of the osmotic pressure provides a measure for the latter, with

$$A_2 M = \frac{\pi N_A}{4} \frac{L\, d_T}{M_L} \tag{10}$$

where $M_L = M/L$ is the mass per unit length for a chain with molecular weight M and contour length L [26, 37, 43]. The experimental results for solutions of PBZT in MSA give $d_T \approx \kappa^{-1}$, where the Debye electrostatic screening length κ^{-1} is related to the ionic strength I_o and the Bjerrum length L_B by

$$\kappa^{-1} \approx (8\pi N_A L_B I_o)^{-1/2} \tag{11}$$

($L_B \approx 0{\cdot}9$ nm for MSA). Owing to the relatively high ionic strength of MSA due to self-protonation ($I_o \approx 10^{-5}$ mol ml^{-1} for monovalent solute), $\kappa^{-1} \approx 2$ nm for PBZT in dilute solutions in MSA. As a consequence, electrostatic intermolecular interactions are essentially completely screened for dilute solutions of PBZT in MSA—that is not true for solutions of PBZT in protic acids of lower ionic strength [43–45]. The cations produced on protonation of the polymer will increment I_o over its infinite dilution limit $(I_o)^{\circ}$ by $\Delta I \approx \nu_p c/2m_o$ for polymer concentration c, with ν_p the charge per polymer repeat unit ($\nu_p \approx 3$ for dilute solutions of PBZT), leading to a decrease in κ^{-1}. In moderately concentrated nematic solutions, the mean distance $\langle d \rangle$ between rods

in the direction orthogonal to the rod axes is approximately $\{M_L/(2\sqrt{3})cN_A\}^{1/2}$, with M_L the mass per unit length of the polymer, or $\langle d \rangle \approx 1{\cdot}5$ nm for the concentrations used here. Since $\langle d \rangle \approx \kappa^{-1}$, electrostatic interactions should be important in the moderately concentrated nematic solutions. The relatively small value for c_{NI}, and the observation that c_{NI} decreases (at fixed temperature) as the ionic strength of the solvent is decreased for solutions of PBZT in protic acids [46] support the postulate that electrostatic interactions among the polycations may be important in certain properties in the solutions of PBZT in MSA in the nematic state, whereas, for example, they may have little effect on the viscosity of isotropic moderately concentrated solutions of PBZT [47, 48].

The electrostatic interactions elaborated above may give nematic solutions of PBZT in MSA some enhanced short-range translational order orthogonal to the chain axes, with a preferred transverse spacing of order $\langle d \rangle \approx \kappa^{-1}$ between the parallel chains. The X-ray diffraction from solutions of poly(1,4-phenylene-2,6-benzobisthiazole) in polyphosphoric acid in the form of oriented fibres [49] is consistent with this postulate, though the order in such a solution may be affected by complex formation of PBZT with the oligomeric acid moieties [50].

The data on $\eta_T/\Delta\chi$ from the growth of the twist and splay distortions are given in figure 3 as a plot of $\log\{(\eta_T/\Delta\chi)\Delta n/M_w[\eta]\}$ versus c/c_{NI}; here, M_w is the weight average molecular weight and $[\eta]$ is the intrinsic viscosity. Multiplication by Δn is motivated by the assumption that for the rod-like PBZT, $\Delta\chi$ may be given by [2, 5, 6, 51]

$$\Delta\chi \approx (\Delta\chi/\rho)^{\circ} cS \qquad (12)$$

where $(\Delta\chi/\rho)^{\circ}$ is the value of $\Delta\chi/c$ for $S=1$ and $c=\rho$. This form assumes that the anisotropic molecular magnetic susceptibility is invariant with c, similar to the assumption made with respect to the optical polarizability. Thus, the ratio $\Delta n/\Delta\chi$ is expected to be independent of c and S. The division by $M_w[\eta]$ is motivated by the theoretical expression for the distortion viscosities for rodlike chains ($\mu = S, T, B$) [38, 39, 52–54]:

$$\eta_\mu = \eta^{ISO} h_\mu(S) \qquad (13)$$

where η^{ISO} is the hypothetical viscosity for an isotropic solution of infinitely thin rod-like chains at the same volume fraction φ and chain contour length L as the nematic [52, 53]:

$$\eta^{ISO} = \eta_s(\pi N_A/K_\eta)^2 M[\eta](c/c_{NI})^3 \qquad (14)$$

with K_η a constant (≈ 120). The form for η_μ is based on the expression

$$\alpha_i = \eta^{ISO} A_i(S) \qquad (15)$$

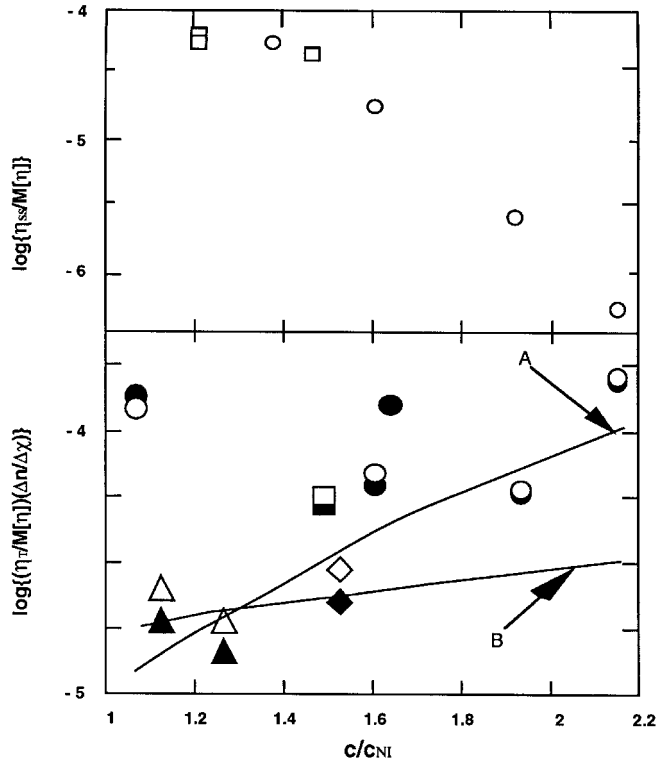

Figure 3. Reduced viscosities as function of concentration relative to the concentration c_{NI} for the order–disorder transition for nematic solutions of PBZT in methane sulphonic acid. The upper panel gives data for the steady state viscosity in the slow flow regime (for which the viscosity is independent of the shear rate). The lower panel gives data on the twist distortion viscosity determined from growth of the distortion in twist (filled) or splay (unfilled) geometries. The symbols are for various samples identifiable by the ratio c/c_{NI} in table 2. The curves A and B represent $\log\{(c/c_{NI})^3\}$ and $\log\{(c/c_{NI})^3 h_T(S)\}$ within arbitrary vertical shifts, respectively, as discussed in the text. Both η_T and η_{ss} are in Pa s, $[\eta]$ is in ml g^{-1}, and $\Delta\chi$ is in Pa T^{-2}.

for the Leslie viscosity coefficients α_i, where the functions A_i have been calculated for a rod-like chain model [38, 39]. Thus, for the twist viscosity, $\eta_T/M[\eta](c/c_{NI})^3 \propto h_T = A_3 - A_2$. Comparison of the experimental data on $(\eta_T/M_w[\eta])(\Delta n/\Delta\chi)$ versus c/c_{NI} with the theoretical expressions is facilitated by a plot of $\log\{(\eta_T/M_w[\eta])(\Delta n/\Delta\chi)\}$ versus c/c_{NI}, so that a plot of $\log\{(c/c_{NI})^3 h_\mu(S)\}$ versus c/c_{NI} may be shifted along the ordinate to compare the two functions within a proportionality constant. As seen in figure 3, the data on $\log\{(\eta_T/M_w[\eta])(\Delta n/\Delta\chi)\}$ versus c/c_{NI} appear to increase more rapidly with increasing c/c_{NI} for the larger c/c_{NI} studied than expected from $(c/c_{NI})^3 h_\mu(S)$, but are similar to the function $(c/c_{NI})^3$. This behaviour is consistent with the approximately constant value of S for these solutions deduced from the dependence of Δn on c/c_{NI},

and could reflect a tendency for enhanced short-range translational order orthogonal to the chain axes noted above.

Although $(\Delta\chi)^{\circ}$ is unknown, an approximation may be deduced from the localized bond (or atom) additivity model to permit estimates of η_T [55]. Based on that model, for the (nearly) planar components comprising the repeat unit of PBZT, $\Delta\chi$ may be approximated from estimates of χ_{OUT}, $\langle\chi\rangle_{IN}$, and $\chi_{\parallel}$, representing the out-of-plane, averaged in-plane, and axial susceptibilities, respectively:

$$\Delta\chi = (\langle\chi\rangle_{IN} - \chi_{OUT})/2 + 3(\chi_{\parallel} - \langle\chi\rangle_{IN})/2 \quad (16)$$

where it anticipated that $\chi_{\parallel} \approx \langle\chi\rangle_{IN}$. Inspection suggests that two moles of benzothiazole comprise the relevant moieties in a PBZT repeat unit, so that $\Delta\chi \approx (\langle\chi\rangle_{IN} - \chi_{OUT})$ using additivity based on $\langle\chi\rangle_{IN}$ and χ_{OUT} per mole of benzothiazole (with the approximation $\chi_{\parallel} \approx \langle\chi\rangle_{IN}$). Although $\langle\chi\rangle_{IN}$ and χ_{OUT} do not appear to be available for benzothiazole, values for phenyleneurea (2-benzimidazolone) should be similar, and are available [55]. Using those data, $(\Delta\chi)^{\circ} \approx 3\,\mathrm{Pa}/T^2$ $(3 \times 10^{-7}\,\mathrm{erg\,G^{-2}\,cm^{-3}})$ for PBZT, so that $\Delta n/\Delta\chi = (\Delta n)^{\circ}/(\Delta\chi)^{\circ}$ is of order unity. Thus, the data in figure 3 give η_T of the same order magnitude as η_{ss}, though the dependence on c/c_{NI} is clearly different.

The enhanced $(\eta_T/M_w[\eta])(\Delta n/\Delta\chi)$ for the sample with the lowest concentration studied may reflect in part some decrease in S, but as shown by the theoretical function $h_T(S)$ versus S given in figure 4, the enhancement appears to be too large to be attributed to that effect alone unless S has changed substantially over a very small span in c/c_{NI}. Some of the enhancement may be related to behaviour noted as a nematic solution of PBZT in MSA is heated to within 20–30°C of its clearing temperature T_{NI},[30] the solution at lowest c/c_{NI} is within that range. The order parameter S decreases slowly as T is increased for a nematic phase of PBZT in MSA, with no other visible change until T approaches the specified temperature, at which point a population of bipolar defects develops with further cooling. The defects appear to comprise a slightly disordered phase within the otherwise well-ordered and defect-free nematic. The conoscopic interference figures are maintained (with somewhat diminished contrast) until a temperature is reached at which the figures can no longer be discerned, and the population of bipolar defects has become large. The defects may represent regions of slightly lower average molecular weight than that of the remaining sample, reflecting anticipated phase segregation by chain length in the nematic phase of rod-like chains polydisperse in chain length [56]. The behaviour at small c/c_{NI} may reflect either unobserved bipolar structures or the effects of regions of incipient formation of these defects.

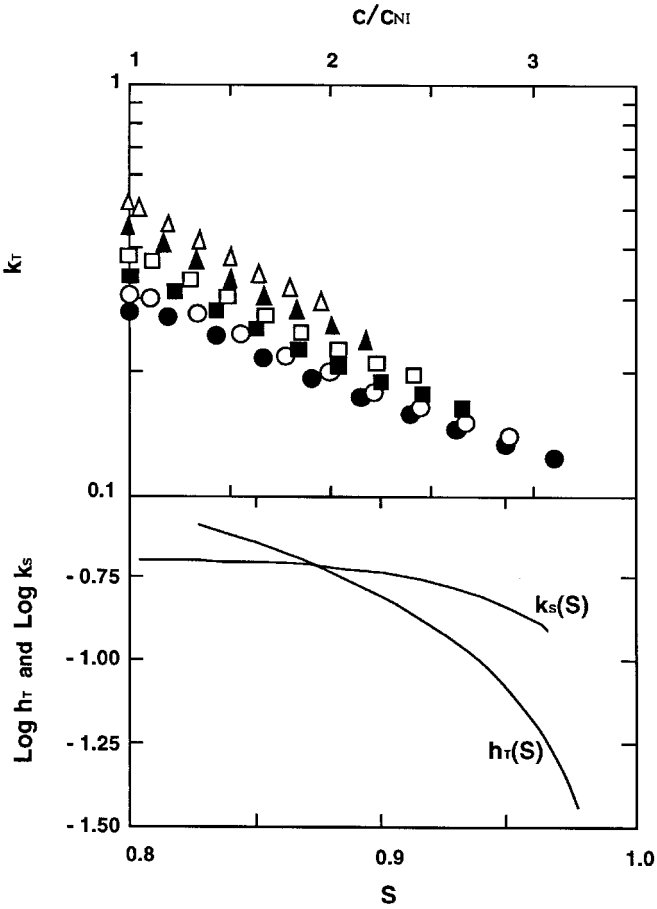

Figure 4. Lower: The theoretical functions $h_T(S)$ and $k_S(S)$ as functions of the order parameter S for a model with a hard-core potential, as discussed in the text. Upper: Theoretical functions for k_T for charged rod-like chains [58, 59], for values of the parameter $h = \kappa d_T)^{-1}$ equal to 0, 0·1, 0·2, 0·3, 0·4 and 0·5 from bottom to top.

It may be noted in figure 3 that the dependence on c/c_{NI} of the steady state viscosity η_{ss} in slow flow (or region II) differs significantly from that of η_T in two respects: $\eta_{ss}/M[\eta]$ decreases with increasing c/c_{NI}, and the change in $\eta_{ss}/M[\eta]$ with c/c_{NI} is much larger than that for $\eta_T/M[\eta]$. This difference reflects the complex nature of the flow in the unaligned, defect-full nematic under study in slow flow [31, 57].

The data on $K_T/\Delta\chi$ and $K_S/\Delta\chi$ from the relaxation of the twist and splay distortions, respectively are given in figure 5 as plots of $\log(K_T/\Delta\chi)\Delta n\}$ and $\log\{(K_S/\Delta\chi)\Delta n\}$ versus c/c_{NI}. Semi-empirical forms for the K_μ for rod-like chains are proportional to $(c/c_{NI})^2$ and to coefficients k_μ ($\mu = S, T, B$) that depend on the order parameter S:

$$K_\mu = (kT/d_T)(c/c_{NI})^2 k_\mu(S) \quad (17)$$

where d_T is the thermodynamic diameter of the rod-like chain, see above. Numerical computations of the k_μ are

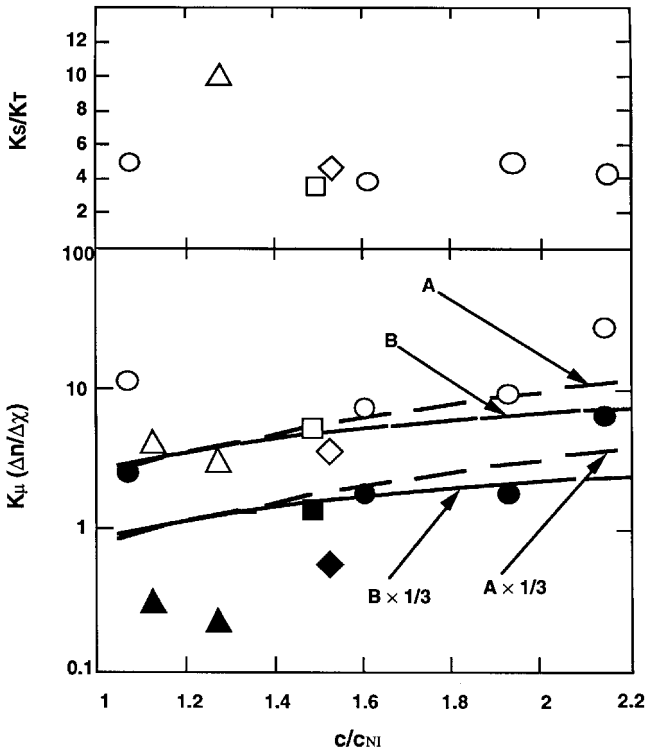

Figure 5. The Frank curvature elasticity determined from relaxation of the distortion of the director field as function of concentration relative to the concentration c_{NI} for the order–disorder transition for nematic solutions of PBZT in methane sulphonic acid. The lower panel gives data on the twist (filled) and splay (unfilled) geometries. The symbols are for various samples identifiable by the ratio c/c_{NI} in table 2. The curves A and B represent $\log\{(c/c_{NI})^3\}$ and $\log\{(c/c_{NI})^3 k_S(S)\}$ within arbitrary vertical shifts, respectively, as discussed in the text, or these functions divided by three, as noted.

available for rod-like chains interacting through a hard-core repulsive [23, 24] or an electrostatic [58, 59] potential. In either case, the calculations give $k_T = k_S/3$ for rod-like chains. The function k_T calculated for polyions for various values of the parameter $h = (\kappa d_T)^{-1}$ is shown in figure 4, with κ^{-1} the Debye screening length; the curve for $h = 0$ corresponds to an uncharged chain with a hard-core repulsive interaction. As may be seen, k_T does not depend markedly on c/c_{NI} (or S, which is a function of c/c_{NI}) for the range of interest here; we note in passing that k_B depends more markedly on h. Consequently, no conclusion may be drawn on whether k_T might be constant for the larger c/c_{NI} studied here. The increase in both for the sample with the smallest c/c_{NI} parallels that observed for twist viscosity for the same sample, and may have a similar origin. For most of the samples, K_T/K_S is found to be slightly larger than the value 3 expected for rod-like chains interacting through a hard-core potential; this behaviour will be discussed further after considering the temperature dependence found for K_T and K_S in this study.

The data on the temperature dependence of K_T and K_S are displayed in figure 6 as $\log\{K_\mu(T)A_\eta(T)/\eta_T(T)\}$ versus T/T_{NI}, where T_{NI} is the temperature for the order–disorder transition, $A_\eta(T) = W(T^{-1} - T_{ref}^{-1})$, with T_{ref} a reference temperature (295 K) and W set equal to the value 2800 K determined for the temperature dependence of the viscosity of nematic solutions of PBZT in MSA (W is close to the value for the temperature dependence of MSA [48]. As may be seen, $K_S(T)A_\eta(T)/\eta_T(T)$ is essentially independent of temperature, suggesting that $A_\eta(T)$ accounts for most of the temperature dependence of η_T, and that the temperature dependence of $K_S(T)$ is weak. Scaling of η_T with $A_\eta(T)$ is reasonable if S does not depend significantly on temperature. The curve shown in figure 6 with $K_S(T)$ is calculated for a rod-like chain taking account of the variation of c_{NI} with temperature given in figure 7, taken from reference [57]. The

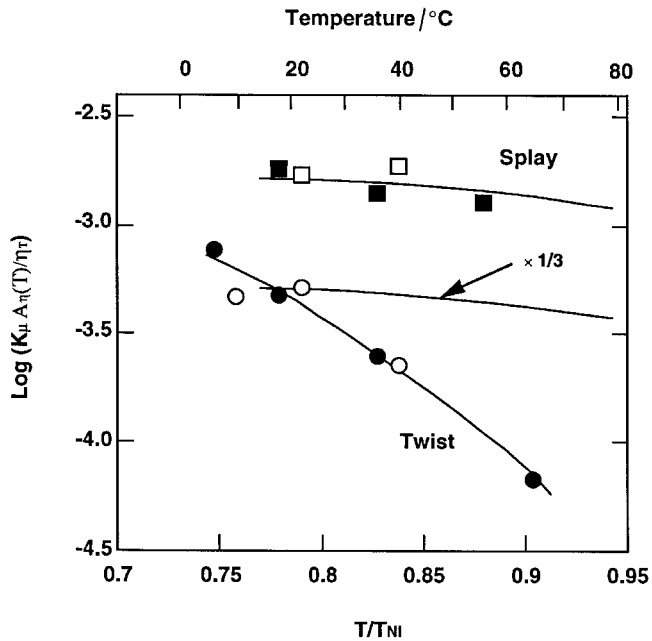

Figure 6. The Frank curvature elasticity determined from relaxation of the distortion of the director field as function of temperature relative to the temperature T_{NI} for the order–disorder transition for nematic solutions of PBZT in methane sulphonic acid for two samples (c/c_{NI} equal to 1·613 and 1·495 at 25°C for the filled and unfilled symbols, respectively). The curve labelled splay is calculated as described in the text. The curve labelled twist is drawn to aid the eye; the curve labelled × 1/3 represents the curve for splay shifted along the ordinate by log(1/3). The function $A_\eta(T) = \exp\{2800[(1/T) - (1/295)]\}$ accounts for the dependence of the steady state viscosity on temperature. As discussed in the text, the estimate for K_T/η_T may be low at the higher temperatures owing to the effects of weakened surface anchoring.

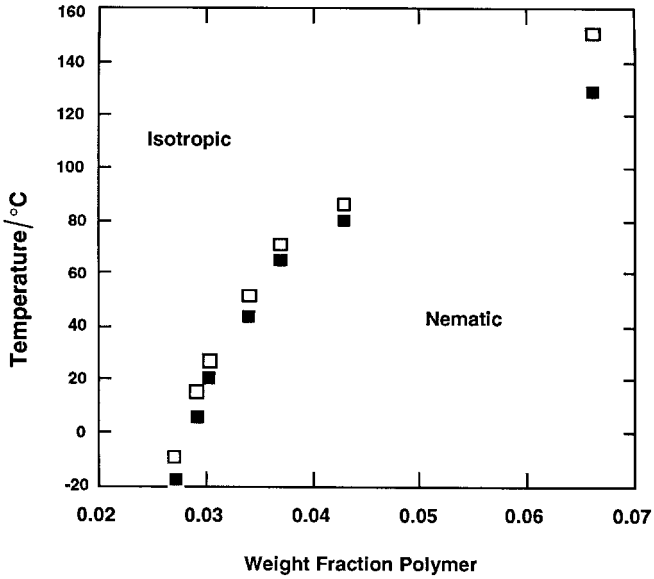

Figure 7. The temperature for the onset of a biphasic ordered and disordered phase and the appearance of a single ordered phase, unfilled and filled squares, respectively, as a function of the weight fraction of polymer for solutions of PBZT in MSA ($L_w = 100$ nm) [46].

experimental trend is consistent with the calculations. By contrast, $K_T(T)A_\eta(T)/\eta_T(T)$, and by inference $K_T(T)$, decreases markedly as T/T_{NI} approaches unity, with $K_S \approx 3K_T$ at the lowest temperatures, as expected for a rod-like chain (either charged or neutral [59]). The ratio K_S/K_T increases to over 10 at the highest temperature owing to the decrease in K_T.

The difference in the temperature dependencies for K_S and K_T is unexpected, and lies outside the frame of the models for the curvature elasticity quoted above, since for them K_S/K_T is constant. That is not true for models for a worm-like chain with persistence length ρ, for which a decrease in ρ gives decreased K_T, with much less effect on K_S [24, 60]. However, the relatively weak increase of c_{NI} with increasing temperature for PBZT in MSA [46, 48] does not suggest any substantial change in the chain conformation over the temperature range of interest. Further, the observation [47] that the temperature dependence of the viscosity of moderately concentrated isotropic solutions of PBZT in MSA is close to that for the solvent indicates that there is essentially no variation of the chain conformation with temperature. A weakening of the surface anchoring with increasing temperature could be implicated in the variation of K_S/K_T with temperature. In the preceding analysis, it has been assumed that the distortion imposed by the external magnetic field relaxes with strong anchoring at the surface. With the solutions studied here, anchoring is presumed to involve polymer adsorption at the glass surface, with the initial orientation at the surface provided by rheological effects on filling the cell [29, 32], giving a preferred direction along the long axis of the cell, consistent with the director orientation in the unperturbed bulk. Fluorescence emission anisotropy studies have shown that a residual surface alignment persists even at temperatures above T_{NI} [31]. Nevertheless, weakening of the anchoring with increased temperature would be reasonable, as has been frequently reported for low molecular weight nematogens [7]. Any such effect would be minimized in the splay geometry, owing to the physical constraint imposed by the wall, in accord with the general finding that polar anchoring tends to be much stronger than azimuthal anchoring for small molecule nematics [7]. Such an effect would result in a low estimate of the twist elastic constant by misinterpretation of the relaxation time constant determined from the rate of rotation of the conoscopic interference figures with time. In particular, a twist occurring over a distance $\xi \ll d$ near the surface, so that the bulk director field is bounded by an effective surface angle ϑ_s relative to the original orientation, would not appreciably affect the rotation of the conoscopic figures (and so would not be detected by that method), but would reduce the torque driving the director field in the bulk to return to its initial orientation, leading to low estimates for K_T/η_T from the rate of relaxation of the conoscopic figures. Thus, the substantial deviation of K_T from $K_S/3$ observed as T/T_{NI} approaches unity could indicate weakening of the surface alignment toward twist distortions. The contribution $F_{surface}$ to the distortion free energy needed to evaluate anchoring effects is calculated using an anchoring energy, often approximated simply as $W_a \sin^2(\vartheta_s)$ in the twist distortion geometry (subscript a denoting an azimuthal parameter, energy per unit area), where ϑ_s is the angle of the director at ξ with respect to the preferred orientation at the surface [7, 8, 61–64]. In this formulation, a length $b_s = 2K_T/W_a$ determines the importance of surface effects, with strong anchoring corresponding to small b_s. In first approximation, if $\xi \ll d$, then a balance of torques gives $\vartheta_s \approx (\pi b_s/2d)\vartheta_{mid}$, so that ϑ_s would increase if W_a decreases with increasing temperature, as has been reported for small molecule nematics [7, 64]. With increasing relaxation time, the distortion in the bulk will slowly relax, reducing ϑ_{mid}, and hence ϑ_s. This coupling complicates the analysis, but qualitatively would lead to a low estimate for K_T/η_T. For example, if it is assumed that the twist at the surface occurs rapidly in comparison with other relaxations, a balance of torques gives

$$K_T \frac{\partial^2 \vartheta}{\partial z^2} = \eta_T \frac{\partial \vartheta}{\partial t} - (W_a/d)\sin(2\vartheta_s). \qquad (18)$$

Then, with the first-order approximation for ϑ_s given above, the estimate for K_T/η_T calculated with neglect of the weakening of the anchoring would be too small by a factor of $\pi/(\pi-2)$, close to the effect seen in figure 6 for the highest temperature. This behaviour may be related to the existence of surface layers in nematic solutions of PBZT deduced from non-linear optical third-harmonic generation (THG) [65]. These surface layers have distinct THG properties, and may exhibit some ordering of the molecular planes parallel to the surface over a distance of more than ten microns. It may be reasonable for such a surface layer to exhibit enhanced twist under the torque imposed by the twisted bulk, especially at elevated temperature. (The total twist induced in the samples at room temperature was approximately identical for each sample.) The surface twist could occur more-or-less abruptly as the temperature is increased from that used to induce the bulk twist distortion, so that subsequent relaxation occurs with a reduced rate, and with a surface twist that gradually reduces with time.

5. Conclusions

The growth of the distortion of the director in an external field, and its subsequent relaxation on removal of the field demonstrates both features that are expected for a nematic phase of rod-like chains, and some that are unexpected. Thus, as expected, the growth of the distortion in two different geometries is the same, as expected, providing an estimate for the twist viscosity (within a proportionality factor of the anisotropy of the diamagnetic susceptibility). The dependence of η_T on the concentration is similar to that expected for rod-like chains, but appears to require that the order parameter is less dependent on concentration than predicted for charged rod-like chains. The latter is in accord with the conclusion reached by direct examination of the order parameter. This behaviour appears to imply a short-range translational order in a direction orthogonal to the chain axis, induced by electrostatic interactions among the polycations produced on protonation of PBZT in the acidic solvent used. The translational order is not in accord with models for charged rod-like chains [58, 59]. The relaxation data give a temperature dependence for the splay curvature elasticity in reasonable accord with theoretical expectations, but that for the twist curvature elasticity shows an unexpectedly strong temperature dependence. This behaviour may reflect a weakening of the surface anchoring with increased temperature, resulting in an erroneously small estimate for K_T by analysis of the relaxation rate with neglect of this effect. Anomalous behaviour is seen in the twist viscosity and the splay and twist curvature elasticities at concentrations close to that for transition to the isotropic phase. The source of this behaviour is unknown, but may be related to molecular weight dispersion in the samples used.

It is a pleasure to acknowledge discussions with Dr Mohan Srinivasarao on several aspects of the work reported especially his remarks on the optical observations of defects in nematic fluids. The generosity of Professor A. P. Koretsky (Biological Sciences Department, CMU) in permitting the use of the magnet in his laboratory is much appreciated. This work, which comprises a portion of the Ph.D. dissertation of B. D., has been supported in part by a grant from the National Science Foundation, Division of Materials Research, Polymers Program.

Appendix

A1. Director field distortion in an external magnetic field

The undistorted director, given by $\mathbf{n}_o = [1,0,0]$, is subjected to a twist distortion with an applied field $\mathbf{H} = [H\cos\vartheta_{mag},\ H\sin\vartheta_{mag}, 0]$ or a splay distortion with an applied field $\mathbf{H} = [H\cos(\varphi_{mag}), 0,\ H\sin(\varphi_{mag})]$. It is assumed that at least for small distortions, the director is given by $\mathbf{n} = [\cos\vartheta(z),\ \sin\vartheta(z), 0]$ in twist distortion and $\mathbf{n} = [\cos\varphi(z), 0, \sin\varphi(z)]$ in splay. That is, the director remains in the plane of the slab in twist, or in a plane defined by $\mathbf{H}$ and $\mathbf{n}_o$ in splay. When expressed in reduced coordinates, a balance of torques in either the splay ($\mu = S$) or twist ($\mu = T$) distortions may be given by [2, 6]

$$m_\mu(\psi)\frac{\partial^2\psi}{\partial z_r^2} + m'_\mu(\psi)\left(\frac{\partial\psi}{\partial z_r}\right)^2 = \Gamma_{mag} + \pi^2\frac{\partial\psi}{\partial t_r}$$

$$\Gamma_{mag} = (\pi h_\mu)^2\sin(\psi-\psi_{mag})\cos(\psi-\psi_{mag})$$

where $\psi = \varphi$ in splay or $\psi = \vartheta$ in twist, $z_r = z/d$, $h_\mu = \mathbf{H}/H_{C,\mu}$, and $t_r = t/\tau_\mu$, with $H_{C,\mu} = (\pi/d)(K_\mu/\Delta\chi)^{1/2}$, ψ_{mag} is the angle of the magnetic field with respect to the undistorted director and $\tau_\mu = d^2\eta_T/\pi^2K_\mu = \eta_T/\Delta\chi H_{C,\mu}^2$. The twist viscosity is implicated in either the splay or twist distortions. Here $2m'_\mu(\psi) = \partial m_\mu(\psi)/\partial\psi$, and the functions m_μ are given by $m_T(\vartheta) = 1$, and $m_S(\varphi) = 1 + \kappa\sin^2\varphi$, with $\kappa = (K_B - K_S)/K_S$. Thus, $m_S(\varphi) \approx 1$ to an approximation that improves as κ tends to zero or φ is small, making the expressions for twist and splay identical in the reduced parameters in that limit.

For the distortions of interest, $\Gamma_{mag} \approx (\pi h_\mu)^2(\psi - \psi_{mag})$, so that at equilibrium,

$$\psi(z,\infty) = \psi_{mag}\left\{1 - \frac{\cosh(\pi h_\mu z_r)}{\cosh(\pi h_\mu/2)}\right\}$$

for either twist or splay (within the stipulated approximation). This expression provides an excellent representation of the relation [66] obtained without resorting

to the approximation for Γ_{mag} for the $\psi(z, \infty)$ of interest here. The growth of the distortion is calculated using the Fourier expansion

$$\psi(z, t) = \psi_{\text{mag}} \sum_{k\ \text{odd}} b_k(h_\mu, t/\tau_\mu) \cos(k\pi z_r)$$

for $k = 1, 3, \ldots$ [67]. The distortion $\psi_{\text{mid}}(h_\mu, \psi_{\text{mag}}, t/\tau_\mu)$ at mid-plane is given by $\psi(0, t)$, with an equilibrium value of

$$\psi_{\max}(h_\mu, \psi_{\text{mag}}) = \psi_{\text{mid}}(h_\mu, \psi_{\text{mag}}, \infty) = \psi_{\text{mag}} \sum_{k\ \text{odd}} b_k(h_\mu, \infty)$$

and

$$b_k(h_\mu, \infty) = \frac{4}{\pi} \frac{(-1)^{(k-1)/2}}{k} \frac{h_\mu^2}{h_\mu^2 + k^2}$$

obtained by standard procedures [68]. Integration over z_r (using the integrating factor $\cos(k\pi z_r)$) after substitution of $\psi_\mu(z, t)$ in the preceding partial differential equation yields a set of ordinary differential equations, which integrate over t to give

$$b_k(h_\mu, t/\tau_\mu) = b_k(h_\mu, \infty)\{1 - \exp[-(h_\mu^2 + k^2)t/\tau_\mu]\}.$$

For $h_\mu \gg 1$, ψ_{mid} tends to ψ_{mag}, and the overall growth of the distortion at mid-plane may be approximated by

$$\psi_{\text{mid}}(h_\mu, \psi_{\text{mag}}, t/\tau_\mu) \approx \psi_{\max}(h_\mu, \psi_{\text{mag}}[1 - \exp(-h_\mu^2 t/\tau_\mu)]$$

making the time constant $\tau_\mu/h_\mu^2 = \eta_T/\Delta\chi H^2$ independent of the Frank elasticity for either splay or twist distortions. A similar analysis of the relaxation of a distortion on removal of the external field following a time t_g of growth of the distortions gives

$$b_k(h_\mu, t/\tau_\mu) = b_k(h_\mu, \infty)\{1 - \exp[-(h_\mu^2 + k^2)t_g/\tau_\mu]\} \times \exp[-k^2(t - t_g)/\tau_\mu]$$

where t is measured from the time the magnetic field is applied, and h_μ refers to the reduced field imposed during the growth of the distortion. To a good approximation,

$$\psi_{\text{mid}}(h_\mu, \psi_{\text{mag}}, (t - t_g)/\tau_\mu) \approx \psi_{\text{mid}}(h_\mu, \psi_{\text{mag}}, t_g/\tau_\mu) \times \exp[-(t - t_g)/\tau_\mu]$$

except possibly for small $t - t_g$.

A2. Conoscopy

The following is a development of the phase retardation $\Delta\varphi$ experienced by a wave propagating through an anisotropic medium, in the limit that the gradients in the refractive index are small and smooth on the scale of the wavelength of light, i.e. only smooth distortions of the director field are admitted. In this case the 'adiabatic approximation' may be applied to describe the propagation of a light wave propagating in the nematic, following is an extension of developments given elsewhere [69, 70]. The coordinate system and the distortion angles are defined as per the schematic diagram.

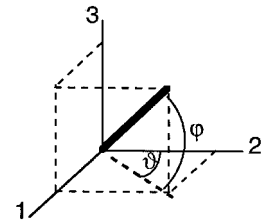

In the adiabatic approximation, the moduli k_i of the wavevector $\mathbf{k} = [k_1, k_2, k_3]$ may be expressed as

$$\lambda^2\left[\left(\frac{k_1}{n_1}\right)^2 + \left(\frac{k_2}{n_2}\right)^2 + \left(\frac{k_3}{n_3}\right)^2\right] = 1$$

where axis-1 is along the director, and the $\mathbf{n}$ is in the 12-plane for the initial, undistorted director field $\mathbf{n}_o$. The strategy is to express the local retardation for a wave propagating in a simple geometry, and then to transform this to the cases of interest by successive rotations of the coordinate system to reach the laboratory coordinate system in the back focal plane of the interference microscope used in conoscopy, making use of the adiabatic propagation approximation.

In the local coordinates, for the o-wave, $n_1 = n_2 = n_3 = n_o$, and for the e-wave, $n_1 = n_o$ and $n_2 = n_3 = n_E$. On rearrangement, the difference Δk_3 between moduli k_3 for these two waves is given by [69]

$$\Delta k_3 = \left(\frac{\Delta n}{\lambda}\right)\left\{1 - 2\left(\frac{\lambda}{2n_O}\right)^2 k_1^2 + 2\frac{n_O}{n_E}\left(\frac{\lambda}{n_O}\right)^2 k_2^2\right\}.$$

If the nematic is undistorted, then the laboratory and local frames are identical, and the retardation in the k_1k_2-plane, which is the back-focal plane in the microscope, is given by

$$\begin{aligned}\Delta\varphi &= \int_{-d/2}^{d/2} d(3)\Delta k_3 \\ &= \left(\frac{d\Delta n}{\lambda}\right)\left\{1 - 2\left(\frac{\lambda}{2n_O}\right)^2 k_1^2 + 2\frac{n_O}{n_E}\left(\frac{\lambda}{n_O}\right)^2 k_2^2\right\} \\ &\approx \left(\frac{d\Delta n}{\lambda}\right)\left\{1 - 2\left(\frac{\lambda}{2\tilde{n}}\right)^2 k_1^2 + 2\left(\frac{\lambda}{2\tilde{n}}\right)^2 k_2^2\right\}\end{aligned}$$

where both n_O and n_E have been replaced by $\tilde{n} = (n_O + n_E)/2$ in the term in brackets in the approximate form. This describes curves of constant phase retardation as nested hyperboli in the k_1k_2-plane, giving rise to the characteristic fringe pattern observed in conoscopy. The spacings of the dark fringes along the director and orthogonal to the director provide a convenient means to determine the birefringence from the approximate

form, or the individual values of n_O and n_E using the full expression [69].

In a pure tilt distortion **n** is tilted by angle φ from axis 1, but remains in the 13-plane. A transformation to a coordinate system with the ξ axis along **n**, the z axis perpendicular to **n**, and in the 13-plane, and the 2 axis renamed to be the η axis (to follow the notation of reference [70]) gives:

$$k_1 = k_\xi \cos\varphi + k_Z \sin\varphi,$$
$$k_2 = k_\eta,$$

and

$$k_3 = k_\xi \sin\varphi - k_Z \cos\varphi.$$

Then, the difference between kz for the e-wave and the o-wave is given by

$$\Delta k_Z \approx \left(\frac{\Delta n}{\lambda}\right)\left\{(1+\cos 2\varphi)/2 - \frac{\lambda}{2\tilde{n}}k_\xi \sin 2\varphi + \left(\frac{\lambda}{2\tilde{n}}\right)^2 [(3-\cos 2\varphi)k_\eta^2 + (1-3\cos 2\varphi)k_\xi^2]\right\}$$

with the approximation signifying the use of $\tilde{n}$ inside the brackets. With ϑ a smooth function of z, integration through the slab gives the retardation in the $k_\eta k_\xi$-plane as

$$\Delta\varphi \approx \left(\frac{d\Delta n}{\lambda}\right)\left\{\frac{1}{2}(1+\langle\cos 2\varphi\rangle) - \frac{\lambda}{2\tilde{n}}\langle\sin 2\varphi\rangle k_\xi - \left(\frac{\lambda}{2\tilde{n}}\right)^2 (3\langle\cos 2\varphi\rangle - 1)k_\xi^2 + \left(\frac{\lambda}{2\tilde{n}}\right)^2 (3-\langle\cos 2\varphi\rangle)k_\eta^2\right\}$$

which describes hyperboli centred at $k_\eta = 0$ and $k_\xi = (\tilde{n}/\lambda)\langle\sin 2\varphi\rangle/(1-3\langle\cos 2\varphi\rangle)$. In these coordinates, the director has no component along the η axis, and the centre of the fringe pattern is shifted along the ξ axis, parallel to $\mathbf{n}_o$. The ratio of the observed displacement Δ of the centre of the fringe pattern of the radius R of the illuminated area is then given by

$$\frac{\Delta}{R} \approx C_\Delta \left(\frac{\tilde{n}}{\Gamma_{NA}}\right)\sin(\varphi_{mid})$$

and

$$C_\Delta = \langle\sin 2\varphi\rangle/\sin(\varphi_{mid})(3\langle\cos 2\varphi\rangle - 1)$$

with Γ_{NA} the numerical aperture of the objective lens. Thus, for magnetic distortion in a weak field ($h \ll 1$ so that $\varphi = \varphi_{mid}\cos(\pi z/d)$), $C_\Delta \approx 0{\cdot}65$. For distortion in a strong field ($h \gg 1$), $C_\Delta \approx 1$.

To include a twist distortion along with the splay, a new coordinate system is introduced, with its y axis rotated by ϑ from the ξ axis, the x axis rotated by ϑ from the η axis, and the z axis unchanged such that the projection of **n** on the $\eta\xi$-plane is twisted by angle ϑ from the ξ axis (to follow reference [70] notation):

$$k_\eta = k_x \cos\vartheta - k_y \sin\vartheta,$$
$$k_\xi = k_x \sin\vartheta + k_y \cos\vartheta$$

and

$$k_z = k_z.$$

The x, y-plane then represents the laboratory plane viewed in the back-focal plane of the microscope, and the difference between the k_z for the e-wave and the o-wave in this plane becomes (correcting a typographical error in reference [70])

$$\Delta k_Z \approx \left(\frac{\Delta n}{\lambda}\right)\left\{\frac{1}{2}(1+\cos 2\varphi) - \frac{\lambda}{2\tilde{n}}k_x \sin 2\varphi \sin\vartheta - \frac{\lambda}{2\tilde{n}}k_y \sin 2\varphi \cos\vartheta + \left(\frac{\lambda}{2\tilde{n}}\right)^2 [(3-\cos 2\varphi)\cos^2\vartheta + (1-3\cos 2\varphi)\sin^2\vartheta]k_x^2 + \left(\frac{\lambda}{2\tilde{n}}\right)^2 [(3-\cos 2\varphi)\sin^2\vartheta + (1-3\cos 2\varphi)\cos^2\vartheta]k_y^2 + 2\left(\frac{\lambda}{2\tilde{n}}\right)^2 [(1-3\cos 2\varphi) - (3-\cos 2\varphi)]\sin\vartheta\cos\vartheta k_x k_y\right\}.$$

With both φ and ϑ smooth functions of z, integration through the slab gives the retardation in the $k_x k_y$-plane as

$$\Delta\varphi = \left(\frac{d\Delta n}{\lambda}\right)\left\{\frac{1}{2}(1+\langle\cos 2\varphi\rangle) - \frac{\lambda}{2\tilde{n}}\langle\sin 2\varphi \sin\vartheta\rangle k_x - \frac{\lambda}{2\tilde{n}}\langle\sin 2\varphi\cos\vartheta\rangle k_y + \left(\frac{\lambda}{2\tilde{n}}\right)^2 \langle(3-\cos 2\varphi)\cos^2\vartheta + (1-3\cos 2\varphi)\sin^2\vartheta\rangle k_x^2 + \left(\frac{\lambda}{2\tilde{n}}\right)^2 \langle(3-\cos 2\varphi)\sin^2\vartheta + (1-3\cos 2\varphi)\cos^2\vartheta\rangle k_y^2 + 2\left(\frac{\lambda}{2\tilde{n}}\right)^2 \langle[(1-3\cos 2\varphi) - (3-\cos 2\varphi)]\sin\vartheta\cos\vartheta\rangle k_x k_y\right\}.$$

where the brackets $\langle \ldots \rangle$ signify an integration through the slab. This describes a fringe pattern of nested hyperboli, with the centre of the pattern shifted by a certain distance Δ from the optic axis of the microscope, and lying along a line at an angle Ω to $\mathbf{n}_0$. To evaluate Ω, which may be determined by examination of the conoscopic image, it is convenient to rotate k_x and k_y by Ω to new axes k_X and k_Y such that

$$k_x = k_X \cos\Omega + k_Y \sin\Omega,$$

$$k_y = -k_X \sin\Omega + k_Y \cos\Omega$$

and

$$k_z = k_z.$$

Then, Ω is determined as the value required to reduce the coefficient of the term in $k_X k_Y$ the new coordinates to zero. Thus, solving implicitly for Ω:

$$\tan 2\Omega = \frac{\langle [(1-3\cos 2\varphi)-(3-\cos 2\varphi)]\sin 2\vartheta \rangle}{\langle [(1-3\cos 2\varphi)-(3-\cos 2\varphi)]\cos 2\vartheta \rangle}.$$

This reduces to the relation of Cladis [69] if there is no tilt distortion ($\varphi = 0$):

$$\Omega = \frac{1}{2}\operatorname{atan}\left(\frac{\langle \sin 2\vartheta \rangle}{\langle \cos 2\vartheta \rangle}\right) = C_\Omega \vartheta_{\text{mid}}$$

and

$$C_\Omega = \operatorname{atan}\{\langle \sin 2\vartheta \rangle / \langle \cos 2\vartheta \rangle\}/2\vartheta_{\text{mid}}$$

Thus, for magnetic distortion in a weak field ($h \ll 1$ so that $\vartheta = \vartheta_{\text{mid}} \cos(\pi z/d)$), $C_\Omega = 0{\cdot}64$. For distortion in a strong field ($h \gg 1$), $C_\Omega \approx 1$.

References

[1] de Gennes, P.-G., 1967, *Physics*, **3,** 37.
[2] Chandrasekhar, S., 1977, *Liquid Crystals* (Cambridge Press, Oxford, UK).
[3] Chandrasekhar, S., and Ranganath, G. S., 1986, *Adv. Physics*, **35,** 507.
[4] Leslie, F. M., 1979, *Adv. Liq. Cryst.*, **4,** 1.
[5] de Gennes, P. G., and Prost, J., 1993, *The Physics Of Liquid Crystals* (New York: Oxford University Press).
[6] de Gennes, P.-G., 1974, *The Physics Of Liquid Crystals* (Oxford, UK: Clarendon Press).
[7] Jérôme, B., 1991, *Rep. Prog. Phys.*, **54,** 391.
[8] Kléman, M., 1983, *Points, Lines And Walls* (New York: John Wiley & Sons).
[9] Deuling, H. J., 1978, *Liquid Crystals*, Vol. 14, edited by L. Liebert (Academic Press), p. 77.
[10] Duke, R. W., and DuPré, D. B., 1974, *J. chem. Phys.*, **60,** 2759.
[11] Sridhar, C. G., Hines, W. A., and Samulski, E. T., 1974, *J. chem. Phys.*, **61,** 947.
[12] Martins, A. F., Esnault, P., and Volino, F., 1986, *Phys. Rev. Lett.*, **57,** 1745.
[13] Tsvetkov, V. N., and Kolomiets, I. P., 1988, *Eur. Polym. J.*, **24,** 379.
[14] Tsvetkov, V. N., and Kolomiets, I. P., 1988, *Mol. Cryst. liq. Cryst.*, **157,** 467.
[15] Tsvetkov, V. N., Kolomiets, I. P., Stepchenkov, A. S., Alimov, S. V., Bilibin, A. Y., and Skorokhodov, S. S., 1989, *Vysokomol. Soedin., Ser. A*, **31**, 700.
[16] Wagner, N. J., and Walker, L. N., 1994, *Macromolecules*, **27,** 5979/86.
[17] Van Eck, D. C., and Perdeck, M., 1978, *Mol. Cryst. liq. Cryst. Lett.*, **49,** 39.
[18] Van der Meulen, J. P., and Zijlstra, R. J. J., 1984, *J. Phys. (Paris)*, **45,** 1627.
[19] van der Meulen, J. P., and Zijlstra, R. J. J., 1984, *J. Phys. (Paris)*, **45,** 1347.
[20] Fellner, H., Franklin, W., and Christensen, S., 1975, *Phys. Rev. A*, **11,** 1440.
[21] Se, K., and Berry, G. C., 1987, *Reversible Polymer Gels and Related Systems*, edited by P. S. Russo (Am. Chem. Soc. Symposium Series), p. 129.
[22] Lee, S.-D., and Meyer, R. B., 1988, *Phys. Rev. Lett.*, **19,** 2217.
[23] Lee, S.-D., and Meyer, R. B., 1990, *Liq. Cryst.*, **7,** 15.
[24] Lee, S.-D., and Meyer, R. B., 1991, *Liquid Crystallinity In Polymers*, edited by A. Ciferri (VCH Publications), p. 343.
[25] Desvignes, N., Suresh, K. A., and Berry, G. C., 1993, *J. Appl. Polym. Sci.*: Polym. Symp., **52,** 33.
[26] Yamakawa, H., 1971, *Modern Theory of Polymer Solutions* (New York: Harper and Row).
[27] Berry, G. C., Metzger, P., and Cotts, D. B., 1981, *British Polymer J.*, **13,** 47.
[28] Asada, T., 1982, *Polymer Liquid Crystals*, edited by A. Ciferri, W. R. Krigbaum and R. B. Meyer (Academic Press), Chap. 9.
[29] Srinivasarao, M., and Berry, G. C., 1992, *Mol. Cryst. liq. Cryst.*, **223,** 99.
[30] Srinivasarao, M., 1990, Ph.D. Dissertation, Carnegie Mellon University.
[31] Diao, B., Matsuoka, K., and Berry, G. C., 1995, *Keynote Lectures In Selected Topics In Polymer Science*, edited by E. Riande (Consejo Superior de Investigaciones Científicas), p. 191.
[32] Srinivasarao, M., and Berry, G. C., 1991, *J. Rheol.*, **35,** 379.
[33] Mattoussi, H., Srinivasarao, M., Kaatz, P. G., and Berry, G. C., 1992, *Macromolecules*, **25,** 2860.
[34] Penz, P. A., 1971, *Mol. Cryst. liq. Cryst.*, **15,** 141.
[35] Rey, A. D., and Denn, M. M., 1989, *Liq. Cryst.*, **4,** 409.
[36] Lee, S-D., 1987, *J. chem. Phys.*, **87,** 4972.
[37] Berry, G. C., 1994, *Adv. Polym. Sci.*, **114,** 233.
[38] Kuzuu, N., and Doi, M., 1983, *J. Phys. Soc. Jpn.*, **52,** 3486.
[39] Kuzuu, N., and Doi, M., 1984, *J. Phys. Soc. Jpn.*, **53,** 1031.
[40] Odijk, T., 1986, *Liq. Cryst.*, **1,** 553.
[41] Lee, C. C., Chu, S.-G., and Berry, G. C., 1983, *J. Polym. Sci.: Polym. Phys. Ed.*, **21,** 1573.
[42] Fan, S. M., Luckhurst, G. R., and Picken, S. J., 1994, *J. chem. Phys.*, **101,** 3255.
[43] Sullivan, V. J., and Berry, G. C., 1995, *Intl. J. Polym. Anal. Charac.*, **2,** 55.
[44] Metzger Cotts, P., and Berry, G. C., 1983, *J. Polym. Sci.: Pt. B: Polym. Phys. Ed.*, **21,** 1255.
[45] Wong, C. P., Ohnuma, H., and Berry, G. C., 1978, *J. Polym. Sci.: Polym. Symp.*, **65,** 173.

[46] Tsai, H. H., 1983, Ph.D. Dissertation, Carnegie Mellon University.
[47] Chu, S.-G., Venkatraman, S., Berry, G. C., and Einaga, Y., 1981, *Macromolecules*, **14,** 939.
[48] Venkatraman, S., Berry, G. C., and Einaga, Y., 1985, *J. Polym. Sci.: Polym. Phys. Ed.*, **23,** 1275.
[49] Radler, M. J., Landes, B. G., Nolan, S. J., Broomall, C. F., Chritz, T. C., Rudolf, P. R., Mills, M. E., and Bubeck, R. A., 1994, *Polym. Mat. Sci. Eng. Preprints, Am. Chem. Soc.*, **71,** 328.
[50] Charlet, A. F., and Berry, G. C., 1989, *Polymer*, **30,** 1462.
[51] Picken, S. J., 1990, *Macromolecules*, **23,** 464.
[52] Berry, G. C., 1989, *The Materials Science And Engineering Of Rigid Rod Polymers*, Vol. 134, edited by W. W. Adams, R. K. Eby and D. E. McLemore (Mat. Res. Soc.), p. 181.
[53] Berry, G. C., 1988, *Mol. Cryst. liq. Cryst.*, **165,** 333.
[54] Lee, S.-D., 1988, *J. chem. Phys.*, **88,** 5196.
[55] Flygare, W. H., 1974, *Chem. Rev.*, **74,** 653.
[56] Flory, P. J., 1984, *Adv. Polym. Sci.*, **59,** 1.
[57] Diao, B., Vijaykumar, S., and Berry, G. C., 1995, *Flow-Induced Structure in Polymers*, Vol. Series 597, edited by A. I. Natatani and M. D. Dadmun (American Chemical Society), p. 274.
[58] Stroobants, A., Lekkerkerker, H. N. W., and Odijk, T., 1986, *Macromolecules*, **19,** 2232.
[59] Vroege, G. J., and Odijk, T., 1987, *J. chem. Phys.*, **87,** 4223.
[60] Odijk, T., 1986, *Macromolecules*, **19,** 2313.
[61] Rapini, A., and Papoular, M., 1969, *Phys. Rev. Lett.*, **66,** 2472.
[62] Ryschenkow, G., and Kléman, M., 1976, *J. chem. Phys.*, **64,** 404.
[63] Faetti, S., Gatti, M., and Palleschi, V., 1986, *Rev. Phys. Appl.*, **21,** 451.
[64] Faetti, S., and Palleschi, V., 1987, *Liq. Cryst.*, **2,** 261.
[65] Mattoussi, H., Berry, G. C., and Patterson, G. D., 1996, *J. Polym. Sci.: Pt. B: Polym. Phys.*, **34,** 925.
[66] Zôcher, H., 1933, *Trans. Faraday Soc.*, **29,** 945.
[67] Pieranski, P., Brochard, F., and Guyon, E., 1973, *J. Phys. (Paris)*, **34,** 35.
[68] Chuchill, R. V., 1941, *Fourier Series And Boundary Value Problems* (New York: McGraw Hill).
[69] Cladis, P. E., 1972, *Phys. Rev. Lett.*, **28,** 1629.
[70] Deuling, H. J., Gabay, M., Guyon, E., and Pieranski, P., 1975, *J. Phys. (Paris)*, **36,** 689.